scientific reports

Check for updates

OPEN

USP39/SMC4 promotes hepatoma cell proliferation and 5-FU resistance

Bo Zhou[1], Jie Li[1], Shuai Wu[1], Haomiao Zhang[1], Yuanbo Luo[1], Jingxiang Chen[2]✉ & Geng Chen[1]✉

Hepatocellular carcinoma (HCC) is a leading cause of cancer-related mortality, characterized by a high rate of postoperative recurrence and poor long-term survival outcomes. Structural maintenance of chromosome 4 (SMC4) is frequently overexpressed in various types of cancer and plays a pivotal role in tumor cell growth, migration, and invasion. Bioinformatics analysis has revealed a significant correlation between the tumor-node metastasis (TNM) stage ($P < 0.01$) and SMC4 expression ($P < 0.05$), and SMC4 was associated with poor prognosis in HCC. Furthermore, SMC4 was identified as an independent prognostic factor for HCC. Ubiquitin-specific peptidase 39 (USP39) was found whether the regulation was observed to affect protein synthesis or stability through bioinformatics analysis and immunoprecipitation. The expression levels and cellular localization of SMC4 and USP39 in hepatoma cells were evaluated using quantitative real-time PCR (qPCR), western blotting, and immunohistochemistry (IHC), all of which indicated significantly elevated expression of USP39 and SMC4 in HCC. The roles of the SMC4/USP39 were further investigated through several assays, including the 3-(4,5-Dimethylthiazol-2-yl) -2,5- diphenyltetrazolium bromide (MTT) assay, 5-ethynyl-2′-deoxyuridine (EdU) incorporation assay, and wound healing assay. The results demonstrated that USP39/SMC4 plays a crucial role in enhancing the viability and proliferation of HepG2 cells. Additionally, bioinformatics analysis identified ZNF207 and TIAL1 as potential target proteins of SMC4. Drug-resistant hepatoma cell lines were established, and both MTT and EdU assays were performed to assess cell viability and proliferation. The results demonstrated that HepG2/5-FU cells regained their sensitivity to 5-FU following the knockdown of SMC4. Additionally, the knockdown of either TIAL1 or ZNF207 also restored 5-FU sensitivity in HepG2/5-FU cells, effectively inhibiting cell viability and proliferation. Our study underscores the significant role of the USP39/SMC4 in HCC development and suggests that SMC4 may contribute to the regulation of drug resistance in hepatoma cell lines, potentially through interactions with TIAL1 and ZNF207.

Keywords Hepatocellular carcinoma, SMC4, USP39, Proliferation, Drug resistance

Hepatocellular carcinoma (HCC) remains a significant global health challenge, ranking as the fifth most common cancer and the fourth leading cause of cancer-related deaths worldwide[1–3]. Annually, over 906,000 new cases of HCC are diagnosed, with approximately 830,000 individuals succumbing to the disease[4,5]. The five-year overall survival rate for HCC patients is alarmingly low, estimated at less than 20%[6,7]. While surgical intervention remains a cornerstone of treatment, extended survival for patients may be achieved through additional therapies such as local radiofrequency ablation, vascular chemoembolization, radiation, and chemotherapy[8–11]. Chemotherapeutic agents like 5-fluorouracil (5-FU), doxorubicin, and platinum-based drugs have shown limited effectiveness in improving patient outcomes[12,13]. Over the past several years, the use of interventional procedures has increased, with 5-FU becoming more commonly utilized in clinical settings[14]. However, the development of drug resistance often undermines the effectiveness of these treatments, especially in advanced or metastatic stages of HCC. Consequently, it is crucial to better understand the mechanisms underlying chemotherapeutic drug resistance and develop strategies to inhibit the progression of HCC.

As a member of the SMC family, the SMC4 protein consists of 1,000 to 1,400 amino acids, with a molecular weight ranging from 110 to 170 kDa[15,16]. It features a moderately conserved hinge region, highly conserved N-

[1]Department of Hepatobiliary Surgery, Daping Hospital, Army Medical University, No. 10, Changjiang Road, Daping, Yuzhong District, Chongqing 400042, China. [2]Department of Hepatobiliary Surgery, The Ninth People's Hospital of Chongqing, No. 1 Yueya Village, Beibei District, Chongqing 400700, China. ✉email: 18436572@qq.com; chengeng@tmmu.edu.cn

and C-terminal domains, and a coiled-coil helix domain that connects the N-terminal and C-terminal regions. SMC4 has been shown to play a crucial role in DNA damage repair, DNA recombination, and chromosome condensation[17–19]. In oncology, SMC4 is overexpressed in several cancer types, including colorectal cancer, HCC, prostate cancer, lung adenocarcinoma, and endometrial cancer, etc[20–25]. Its involvement in regulating tumor cell growth, migration, and invasion highlights the importance of SMC4 in tumor aggressiveness[26]. As a result, SMC4 is considered a promising therapeutic target in HCC[27–29]. However, the precise mechanism by which SMC4, particularly when deubiquitinated, contributes to the progression of HCC remains unclear. This study aims to provide new insights into the role of SMC4 in the development of chemoresistance in HCC and to further elucidate the underlying processes involved in HCC progression.

Materials & methods

Data acquisition

The genetic datasets and clinical samples used in this study were obtained from the GSE14520 database (https://www.ncbi.nlm.nih.gov/geo/query/acc.cgi?acc=GSE14520) and the Liver Hepatocellular Carcinoma (TCGA-LIHC) dataset (https://www.cbioportal.org/study/clinicalData?id=lihc_TCGA-LIHC_pan_can_atlas_2018). This study focused on examining the alterations in the expression and prognosis of SMC4 in tumors from Chinese HCC patients with Hepatitis B Virus (HBV) infection (CHCC-HBV), as reported in the following publication: https://pubmed.ncbi.nlm.nih.gov/31585088/. Additionally, the (http://plmd.biocuckoo.org/view.php?id=0037417#sequence) GPS-Uber Database (https://gpsuber.biocuckoo.cn/) was used to explore the amino acid modifications and potential ubiquitination modification sites of SMC4.

Functional enrichment analysis

To conduct comprehensive functional enrichment studies, we utilize the enrichGO function from the 'clusterProfiler' R package for Gene Ontology Biological Process (GOBP) analysis and subsequently generate a bubble plot with the 'ggplot2' R package. Gene Set Enrichment Analysis (GSEA) was performed using the GSEA function of the 'clusterProfiler' R package, utilizing the gene expression profile dataset from patients in GSE14520. GSEA is a computer technique used to determine whether there are statistically significant differences between two biological states in terms of a specific collection of genes. The result was considered statistically significant if the adjusted p-value was less than 0.05. The RFS and OS of significant genes in the GSE14520 dataset were analyzed using the R language survival package for univariate / multivariate COX analysis. LASSO regression analysis was performed using the 'glmnet' R package.

Risk model construction based on SMC4-related genes

To examine the expression of genes associated with SMC4 in HCC, we used Pearson correlation analysis to assess the expression of SMC4 in tumor tissue samples. In addition, we analyzed the relationship between SMC4 and SMC4-related genes in the GSE14520 database. The genes that positively correlated with SMC4 were examined using GOBP, and the differential expression of SMC4 (high and low) was assessed using the 'Limma' R package. Moreover, gene functional enrichment analysis was conducted using the GSEA program. To investigate genes strongly associated with prognosis, particularly recurrence-free survival (RFS), we performed univariate Cox analysis on tumor tissue samples from both the GSE14520 and TCGA-LIHC databases. Genes positively correlated with SMC4 expression were compared to those linked to prognosis. LASSO regression analysis was then used to examine the RFS of the selected genes, and multivariate Cox analysis was performed to develop risk models.

Sensitivity analysis of anticancer drugs

We utilized the R package (oncoPredict) to predict the half maximal inhibitory concentration (IC50) values of anticancer drugs based on data from GSE14520 and TCGA-LIHC databases. The analysis evaluated the relationship between patients with high-risk and low-risk scores and their sensitivity to different anticancer drugs, as determined by IC50 values.

Cell culture and clinical samples

Human hepatoma cell lines (97-H, HCCC-9810, Bel-7405, HepG2, Hep3B, LM3, HuH-7) were procured from the Chinese Academy of Sciences (Shanghai, China). A total of ten pairs of HCC and paracancerous tissues were collected from HCC patients prior to therapy. The clinical samples were obtained from the Department of Hepatobiliary Surgery, Daping Hospital between Sep 2022 and Mar 2023. All samples were immediately snap-frozen and stored at -80 °C pending further use.

Quantitative real-time PCR (Polymerase chain Reaction) (qPCR)

Cells and tissues were subjected to RNA extraction using trizol reagent (Invitrogen, Carlsbad, USA) and the RNA Extraction Kit (Invitrogen), following the instructions provided by the manufacturer. The synthesis of cDNA was performed using reverse transcription with the PrimeScript RT kit manufactured by Takara, Japan. We used the SYBR Green PCR master mix (Invitrogen) to run real-time PCR in a PCR machine (Applied Biosystems, USA) using conventional quantitative PCR protocols. The primer sequences used are outlined in Table 1. The control utilized in the experiment was β-actin obtained from Sangon Biotech in Shanghai, China.

Western blotting analysis

We used the total protein extraction kit (AmyJet Scientific Inc., China) to extract total proteins from cultured cells and clinical samples as per the manufacturer's instructions. The proteins were separated using sodium dodecyl sulfate-polyacrylamide gel electrophoresis (SDS-PAGE) and then transferred to polyvinylidene difluoride

Homo	primer sequence (5′--3′)
SMC4-F	TTGTCATGCACTGGACTACATTG
SMC4-R	TTTTTCGCCCATACAGCCATC
USP39-F	GGTTTGAAGTCTCACGCCTAC
USP39-R	GGCAGTAAAACTTGAGGGTGT
ZNF207-F	CCAGCGGCTTCAATAACAAGT
ZNF207-R	GGCCGAGGAAGATTACGTTGAT
TIAL1-F	GTTTCGGTGAACGGTACTACG
TIAL1-R	TCCATTGGCCCCATTGACTAT
β-actin-F	ACCCTGAAGTACCCCATCGAG
β-actin-R	AGCACAGCCTGGATAGCAAC

Table 1. The primer sequences.We have uploaded a new table and corrected.

Clone ID	Target sequences (5'-3')	Match Region	SDR Match
USP39-1	GCCGGGTATTGTGGGACTGAA	673	CDS
USP39-2	GATTTGGAAGAGGCGAGATAA	1660	CDS
ZNF207-1	ATAGCCAAGCTTCCGTCAATA	1696	3'UTR
ZNF207-2	GCAGGTACATAAAGAAACAAT	313	CDS
TIAL1-1	GCATACAAGCAATGACCCATA	693	CDS
TIAL1-2	ATTCATGATAGGCTTCGATTT	1718	3'UTR

Table 2. The SiRNA sequences target sequences. CDS: Coding sequence; 3'UTR: 3' Untranslated Region.

(PVDF) membranes (Millipore, Bedford, MA, USA). The membranes were then incubated overnight at 4 °C with antibodies against SMC4 (Abcam, UK) (1:500), USP39 (Ptgcn, USA) (1:1000), ZNF207(Genetex, USA) (1:500) and TIAL1 (Abcam, UK) (1:1000). Positive protein bands were visualized by exposing the membrane to X-ray films. β-actin (Ptgcn, USA) (1:2000) was used as a control.

Immunohistochemistry (IHC)

The basic procedure for formalin-fixed paraffin-embedded (FFPE) samples is as follows: First, remove the frozen tissue and allow it to reach room temperature, then fix it in 4% paraformaldehyde (PFA) for 48-hour. Next, wash the tissue three times with phosphate buffer solution (PBS), each wash lasting 10 min, proceed with dehydration using increasing concentrations of ethanol (70%, 80%, 90%, and 100%), each for 30 min. After dehydration, immerse the tissue in xylene for 30 min for clearing, then embed it in paraffin at a temperature of 52–54 °C to form conventional Sects. (3–5 μm) and place them on clean glass slides. Finally, bake the slides at 60 °C for 2 h, then store them in a slide cassette and seal at 4 °C for immunohistochemical (IHC) detection.

The paraffin-embedded tissues were cut into 3-um pathological sections. Subsequently, the sections were subjected to dewaxing, hydration, and three 5-minute washes with 1×PBS buffer (0.01 M, pH 7.2). The tissue chip was incubated with primary antibodies (SMC4, 1:100; USP39, 1:200) at 37°C for 1 hour. Following a 3 × 5 minutes PBS washes, each slice was exposed to 50μl of biotin-labeled secondary antibody (1:4000, Abcam) for 10 minutes at the room temperature. Subsequently, freshly prepared 3,3'-diaminobenzidine (DAB) solution was applied to each section, and staining was observed under a microscope at 400× magnification. Positive expression sites were identified by brown-yellow coloration.

Protein stability

Cells were treated with cycloheximide (CHX), a protein synthesis inhibitor, at a concentration of 10 μg/ml for detection purposes. Cycloheximide was introduced to impede protein synthesis at 0, 3, 6, and 12 h prior to cell collection. The presence of SMC4 protein was identified by western blotting, with β-actin serving as the control.

Vector construction and transfection

Following the manufacturer's instructions, cells were cultured in six-well plates and transfected with small interfering RNA (siRNA) using Lipofectamine™ RNAi MAX transfection reagent (GenePharma, China). The siRNA sequences targeting SMC4 were consistent with those utilized in our previous study[20]. Additionally, the SMC4 overexpression vector was purchased from Clontech. The siRNA sequences targeting USP39, ZNF207, and TIAL1 are listed in Table 2.

Co-immunoprecipitation

According to the manufacturer's instructions, co-immunoprecipitation assays were performed using the Pierce Co-immunoprecipitation kit (Pierce, USA). Cultured cells were lysed with 1 ml of cell lysate, and the protein concentration was determined to be 0.5 mg/ml. To the lysate, 4 μl of sample volume and 2 μg of primary antibodies (SMC4) were added, and the mixture was incubated overnight at 4 °C. 20 μl of Protein A + G Agarose

were introduced and delicately agitated for two hours at a temperature of 4 °C. Next, the samples were mixed vigorously with 40 µl of 2× SDS-PAGE loading buffer using a vortex and heated in boiling water for 3–5 min. Subsequently, the samples were subjected to SDS-PAGE and western blotting. β-actin was used as the control.

5-ethynyl-2′-deoxyuridine (EdU)

A total of 5,000 cells were placed in each well of six-well plates. Following a 48 -hour transfection, an equal volume of 2×EdU was introduced to the plates and incubated at 37 °C. Following incubation, the cells were fixed to prepare for immunostaining. The cells were then stained using the Click Additive Solution, and the nuclei were labeled with Hoechst 33,342 dye (Beyotime, China). EdU-positive cells were observed using a fluorescent microscope (Olympus, Japan) at 400× magnification. The experiment was repeated three times.

(3-(4,5-Dimethylthiazol-2-yl)-2,5-diphenyltetrazolium bromide (MTT)

Cellular viability was assessed using the MTT assay. A total of 10,000 cells were seeded into 96-well plates and cultured in a 37 °C, 5% CO_2 cell incubator for 24 h. Subsequently, 50µL of 1×MTT was added to each well and incubated at 37 °C for 4 h. After removing the supernatant, 150µL of DMSO was added to each well. The MTT colorimetric test measured cell proliferation at a wavelength of 570 nm at time points of 0, 12, 24, 48, and 72 h. The experiment was repeated three times.

Wound healing

The wound healing assay was performed to evaluate cellular migration. 1.2×10^6 cells were seeded into 24-well plates and cultured in DMEM (Dulbecco's modified eagle medium) at 37 °C with 5% CO_2. The cells were allowed to grow until they reached a 90–100% confluence level. Subsequently, a scratch was then made in the center of the cell monolayer using a sterile micropipette tip. Photographs were taken at 0 and 48- hour post-scratch using an inverted microscope (Nikon, Japan) at 40× magnification. The experiment was repeated three times.

Establishment of drug-resistant cell lines

To establish drug-resistant cell lines, cells were exposed to various concentrations of 5-fluorouracil (5-FU) (0, 50, 100, 200, 400, 800, and 1,600 nM) for 48-hour. The cell survival rate was determined using the MTT assay. The half-maximal inhibitory concentration (IC50) was calculated using SPSS 24.0 software. 5-FU-resistant cells were obtained by continuous treatment with the IC50 dose of 5-FU for 4 weeks.

Statistical analysis

Statistical analysis was performed using R software (version 4.1.2) and SPSS 24.0 (Inc., Chicago, IL, USA). The differences were considered significant when the *P*-value was less than 0.05.

For comparing continuous variables between two groups, One-Way ANOVA was used to assess the statistical significance of normally distributed variables, with results presented as mean ± standard deviation (SD) (SPSS 24.0). Pearson correlation analysis was performed to calculate the correlation coefficients between different genes. Survival analysis was carried out using the survival package in R, and Kaplan-Meier survival curves were generated to illustrate survival differences. The log-rank test was employed to evaluate the significance of the differences in survival time between the two groups. Univariate and multivariate Cox analyses were conducted to identify independent prognostic factors. (R software (version 4.1.2)).

Results

SMC4 was an independent prognostic factor for the prognosis of HCC

To examine the role of SMC4 in HCC, gene expression data from the GSE14520 dataset were analyzed. This dataset contained paired tumor and non-tumor tissues. After removing samples with incomplete TNM stage information, a total of 219 samples were subjected to Cox analysis and survival prognostic curve analysis, using the Kaplan-Meier plotter (Fig. S1). The univariate Cox regression analysis of OS and RFS revealed a strong correlation between the TNM stage ($P < 0.01$) and SMC4 ($P < 0.05$) with a poor prognosis in HCC (Fig. S1 1 A, C). All variables showing statistical significance in the univariate analysis were incorporated into the multivariate Cox regression model. The multivariate Cox regression analysis for OS and RFS also identified TNM stage ($P < 0.01$) and SMC4 ($P < 0.05$) as independent prognostic factors for both OS and RFS (Fig. S1 B, D). Additionally, Kaplan-Meier curve analysis was used to assess the impact of risk scores on OS and RFS in HCC patients, demonstrating a negative correlation between SMC4 expression levels and both OS and RFS (Fig. S1 E and F).

To further validate these results, we conducted a more detailed analysis of SMC4 expression using the TCGA-LIHC dataset, which included 372 samples (Fig. S2). Consistent with the findings from the GSE14520 dataset, we observed a significant association between SMC4 expression and prognosis in HCC.

The importance of USP39/SMC4 in the prognosis of HCC

In the tumor tissue samples (219 samples) from the GSE14520 dataset, Pearson correlation analysis was used to investigate the relationship between SMC4 expression and other genes ($|cor| >= 0.3$, $P < 0.05$). A total of 1,141 genes were found to be positively correlated with SMC4 expression. Functional enrichment analysis through Gene Ontology (GO) was then performed, identifying twelve significant pathways, which were visualized in a bubble plot (Fig. 1A). Additionally, GSEA was conducted on the same 219 tumor samples from the GSE14520 dataset, and differential expression of SMC4 (classified as high and low) was assessed using the Limma program. Gene functional enrichment analysis was carried out using the clusterProfiler package (GSEA program). The GSEA results revealed a positive correlation between high SMC4 expression and pathways involved in protein-

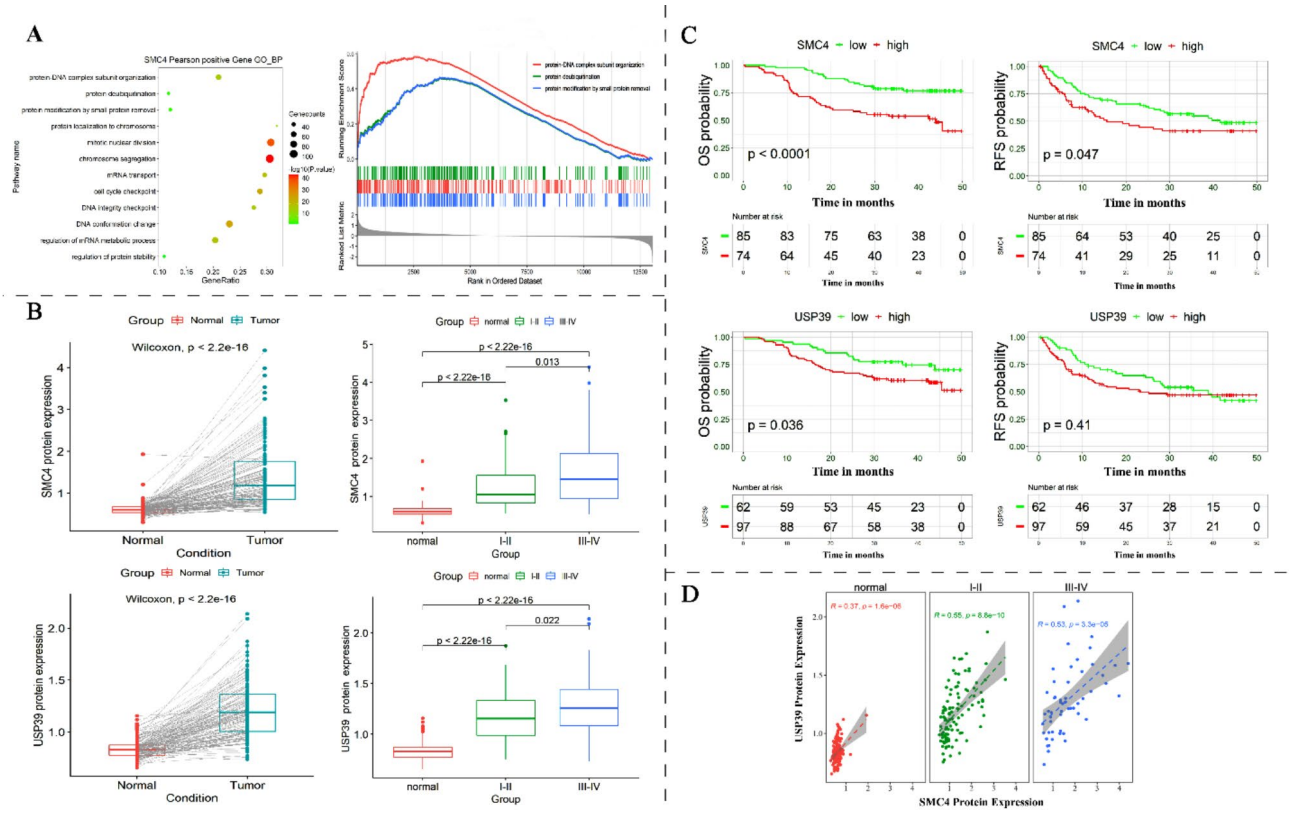

Fig. 1. USP39/ SMC4 may have played an important role in the prognosis of HCC. (**A**). GOBP analysis of the gene set had a positive correlation with SMC4(left); GSEA analysis of the gene set was related to the SMC4(right). (**B**) Wilcoxon analysis of SMC4/USP39 protein in HCC(left); Wilcoxon analysis was also used to study the relationship between the expression of SMC4/USP39 and the stage of HCC (right). (**C**) The relationship between the expression of SMC4/USP39 and OS/RFS by Kaplan-Meier. (**D**) Pearson analysis of the correlation between the expression of SMC4 protein and USP39(The samples were divided into normal control group (normal), tumor (TNM stage I-II), tumor (TNM stage III-IV). (OS, overall survival; RFS, relapse-free survival; GOBP, Gene Ontology Biological Process).

DNA complex subunit organization, protein deubiquitination, and protein modification through small protein removal (Fig. 1A).

Further GOBP and GSEA analyses of genes associated with SMC4 expression in the GSE14520 dataset revealed significant enrichment of the USP family of protein deubiquitination enzymes (USP1, USP3, USP13, USP15, USP33, USP39, USP46). These USP proteins were notably enriched in GOBP (GO:0016579, GO:0070646) and were significantly upregulated in the GSEA analysis (GO:0070646). Furthermore, we performed CHCC-HBV analysis, which indicated that only USP39 protein levels were upregulated in HCC. To further explore the relationship between SMC4 and USP39, we used the Wilcoxon test followed by Bonferroni correction and found a strong association between the high expression of SMC4/USP39 and advanced tumor stage in HCC (Fig. 1B).

Additionally, we investigated the expression of SMC4 in the CHCC-HBV cohorts and performed paired proteomic detection in 159 pairs of HCC and paracancerous tissues. The results demonstrated that SMC4 expression was increased in HCC samples. This elevated expression was associated with shorter OS and RFS (Fig. 1C). At the same time, we assessed the prognostic significance of USP39 in HCC patients using the Kaplan-Meier in the CHCC-HBV cohorts (Fig. 1C). Patients were categorized into high and low USP39 expression groups according to the median value of USP39 expression. The high USP39 expression group exhibited significantly worse OS and RFS than those with low expression. The Pearson correlation analysis demonstrated a positive association between the expression levels of SMC4 and USP39(Fig. 1D), and the results suggested the they were positively correlated in both normal samples and tumor samples, especially the tumor samples with a high correlation coefficient (TNM I-II, $R = 0.55$, $p = 8.8 \times 10^{-10}$; TNM III-IV, $R = 0.53$, $p = 3.3 \times 10^{-5}$).

USP39 /SMC4 were significantly expressed in HCC

To validate the findings from the bioinformatics analysis, we collected ten pairs of HCC tissues and adjacent paracarcinoma tissues. Expression levels of USP39 and SMC4 in HCC tissues were analyzed using qPCR and Western blotting. The results demonstrated a significant increase in the expression levels of both USP39 and SMC4 in HCC tissues compared to paracarcinoma tissues (Fig. 2A). Furthermore, expression levels of USP39 and SMC4 in several hepatoma cell lines (97-H, HCCC- 9810, Bel-7405, HepG2, Hep3B, LM3, HuH-7) (Fig. 2B). Based on the high expression of both SMC4 and USP39, we selected HepG2 cells for further investigation.

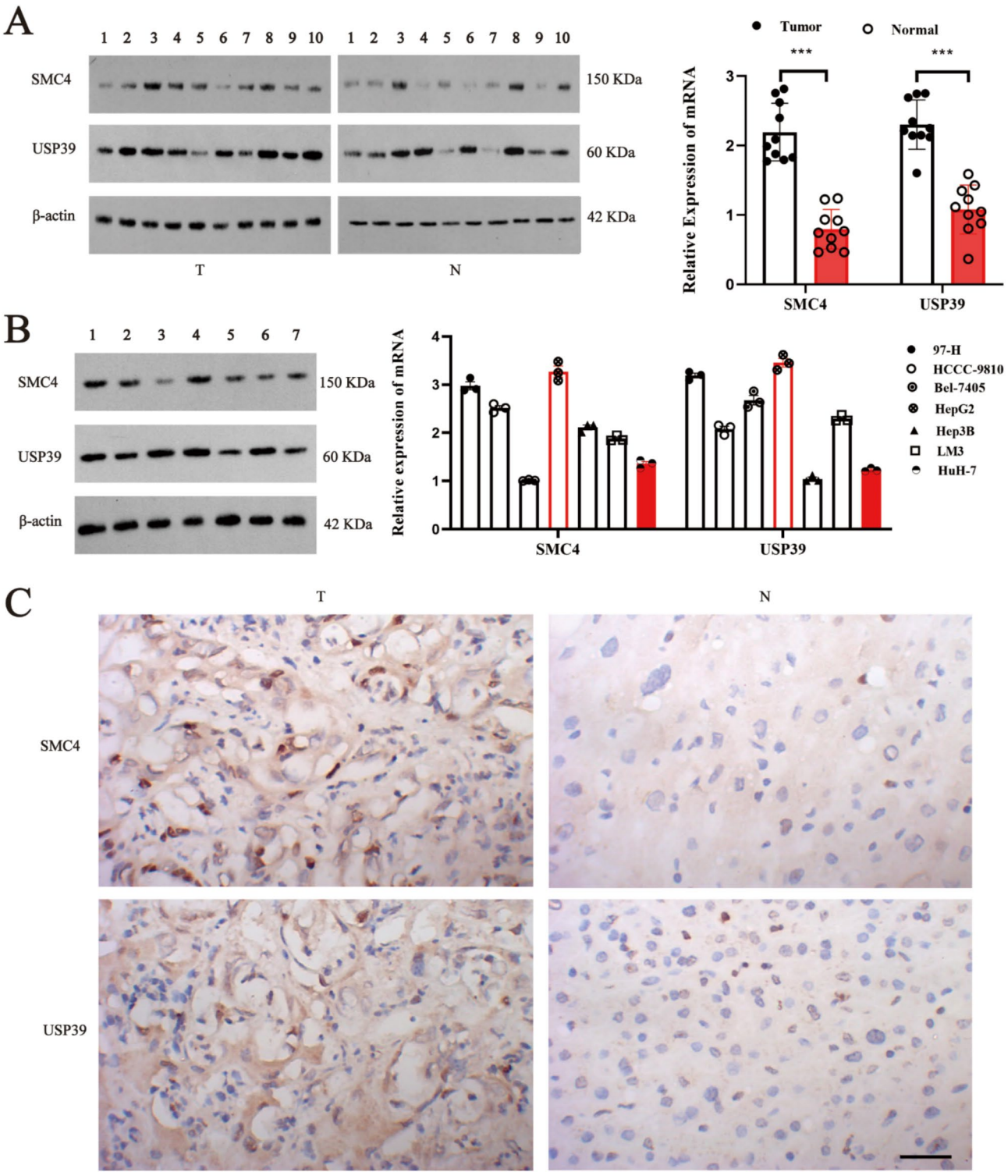

Fig. 2. USP39 /SMC4 were significantly expressed in HCC. (**A**) Western blotting and qPCR were performed to analyze the level of SMC4/ USP39 in HCC tissues. (**B**) Western blotting and qPCR were performed to analyze the level of USP39/SMC4 in hepatoma cell lines (1,97-H;2, HCCC – 9810;3, Bel- 7405; 4, HepG2;5, Hep3B; 6, LM3;7, HuH-7). (**C**) Immunohistochemistry was also used to examine the expression level and localization of USP39/SMC4 in HCC tissues (×400). (Data shown as mean ± SD; *** $P < 0.001$; scale bar: 50 μm).

Immunohistochemistry was performed to examine the expression and localization of USP39 and SMC4. The results indicated a significant increase in both the USP39 and SMC4 in HCC tissues, and SMC4 was observed in both the nucleus and cytoplasm, with a predominant localization in the nucleus, while USP39 was mainly localized in the cytoplasm. (Fig. 2C).

The significance of USP39/SMC4 in promoting the viability and proliferation of HepG2 cells

We conducted a series of experiments to explore the functional roles of USP39 and SMC4 in HCC. Initially, USP39-siRNA was transfected into HepG2 cells, and the expression levels of USP39 and SMC4 were evaluated by qPCR. The findings revealed that SMC4 expression remained unchanged despite the interference of USP39 (Fig. 3A). Further, we used the co-immunoprecipitation analysis to investigate the interaction between USP39 and SMC4, as well as the ubiquitination status of SMC4 (Fig. 3B). The results revealing a binding interaction between USP39 and SMC4, with a significant reduction in SMC4 protein levels in the USP39-siRNA group compared to the control groups. This decrease was attributed to the introduction of USP39-siRNA, which led to increased ubiquitination of SMC4 and a subsequent reduction in SMC4 protein levels. To further validate the role of USP39, a protein stability assay was performed in HepG2 cells, demonstrating that USP39-siRNA accelerated the degradation of SMC4 protein (Fig. 3C). Subsequently, the viability and proliferation of HepG2 cells were evaluated by MTT, EdU, and scratch assays. The viability, proliferation, and motility of HepG2 cells were markedly reduced in the USP39 -siRNA group, where USP39 was suppressed, compared to the control group (Fig. 3D, E). These findings suggest that USP39 plays a crucial role in maintaining the stability of SMC4 by facilitating the removal of ubiquitin, thereby promoting the viability and proliferation of HepG2 cells.

Co-transfection experiments were conducted in HepG2 cells using USP39- siRNA and either SMC4-overexpression (OE) or SMC4-siRNA to further explore the impact on cell phenotype. qPCR and western blotting were performed to verify the efficiency of gene silencing and overexpression. As shown in Fig. 4A, when USP39 was knocked down, SMC4 gene expression remained unchanged, but the SMC4 protein levels decreased. Upon co-transfection of USP39-siRNA and SMC4-OE, USP39 expression was significantly reduced, while SMC4 expression was restored at both the gene and protein levels. MTT, EdU, and scratch assays were performed to evaluate cell viability and proliferation. In Fig. 4B-C, where either USP39 or SMC4 was suppressed, the viability and proliferation of HepG2 cells were reduced. However, in USP39-siRNA + SMC4-OE group, where USP39 was suppressed, and SMC4 was overexpressed, a partial recovery of cell viability and proliferation was observed. These results underscore the critical role of the USP39/SMC4 axis in enhancing the viability and proliferation of HepG2 cells.

The effect of SMC4 on the proliferation of HCC might be mediated by TIAL1/ ZNF207

The tumor tissue samples from the GSE14520 dataset were analyzed through univariate Cox regression to identify genes ($n = 2552$, $P < 0.05$) strongly associated with RFS. Venn analysis revealed a total of 181 genes that were positively correlated with SMC4 and showed significant predictive value for RFS. LASSO regression

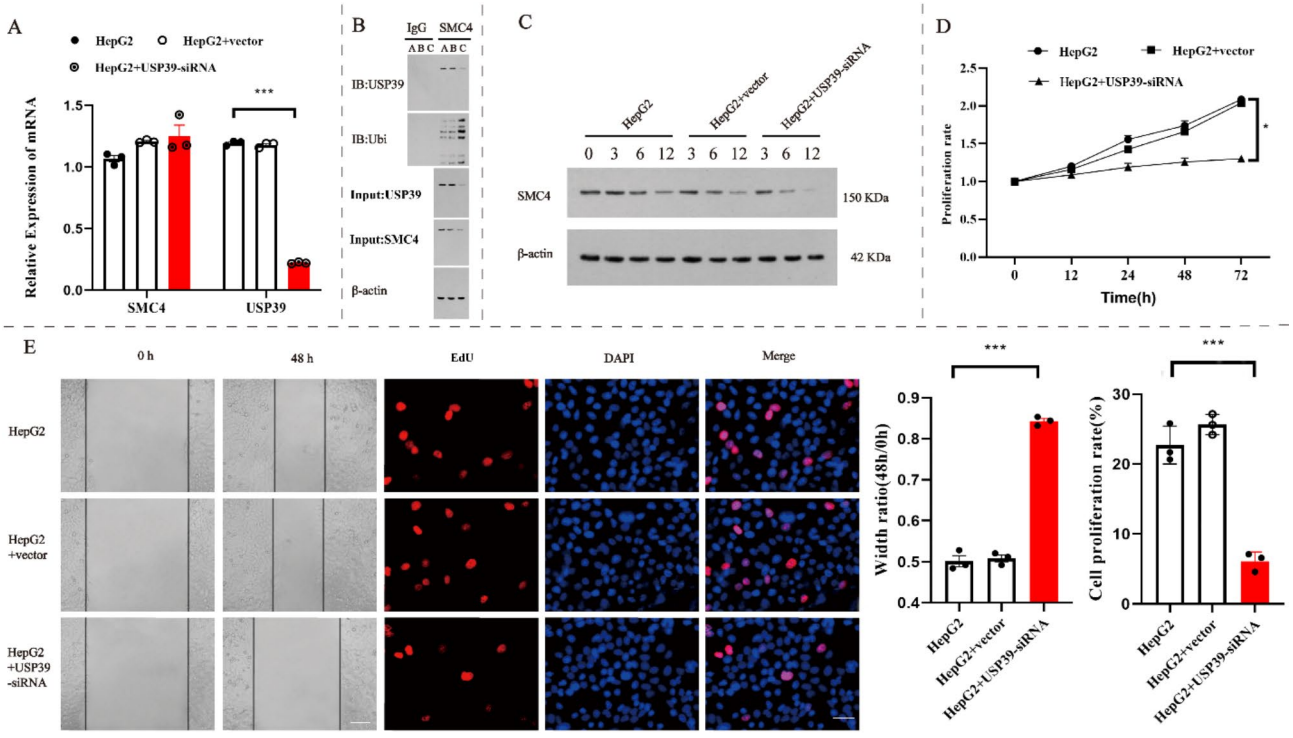

Fig. 3. USP39 could regulate the deubiquitination of SMC4 and affect cell proliferation and viability. (**A**) qPCR was done to detect the expression of USP39 and SMC4 after USP39 was knocked down. (**B**) Co-immunoprecipitation was performed to investigate the relationship between USP39 and SMC4, as well as the ubiquitination level of SMC4. (A, HepG2; B, HepG2 + vector; C, HepG2 + USP39-siRNA). (**C**) The protein stability assay was performed to assess the stability of the SMC4 protein after the USP39 was knocked down. MTT(**D**), Scratch assay, and EdU (E) were used to detect the viability and proliferation of the HepG2 after USP39 knocking down. (Data shown as mean ± SD; * $P < 0.05$, ** $P < 0.01$, *** $P < 0.001$; scale bar: 50 μm).

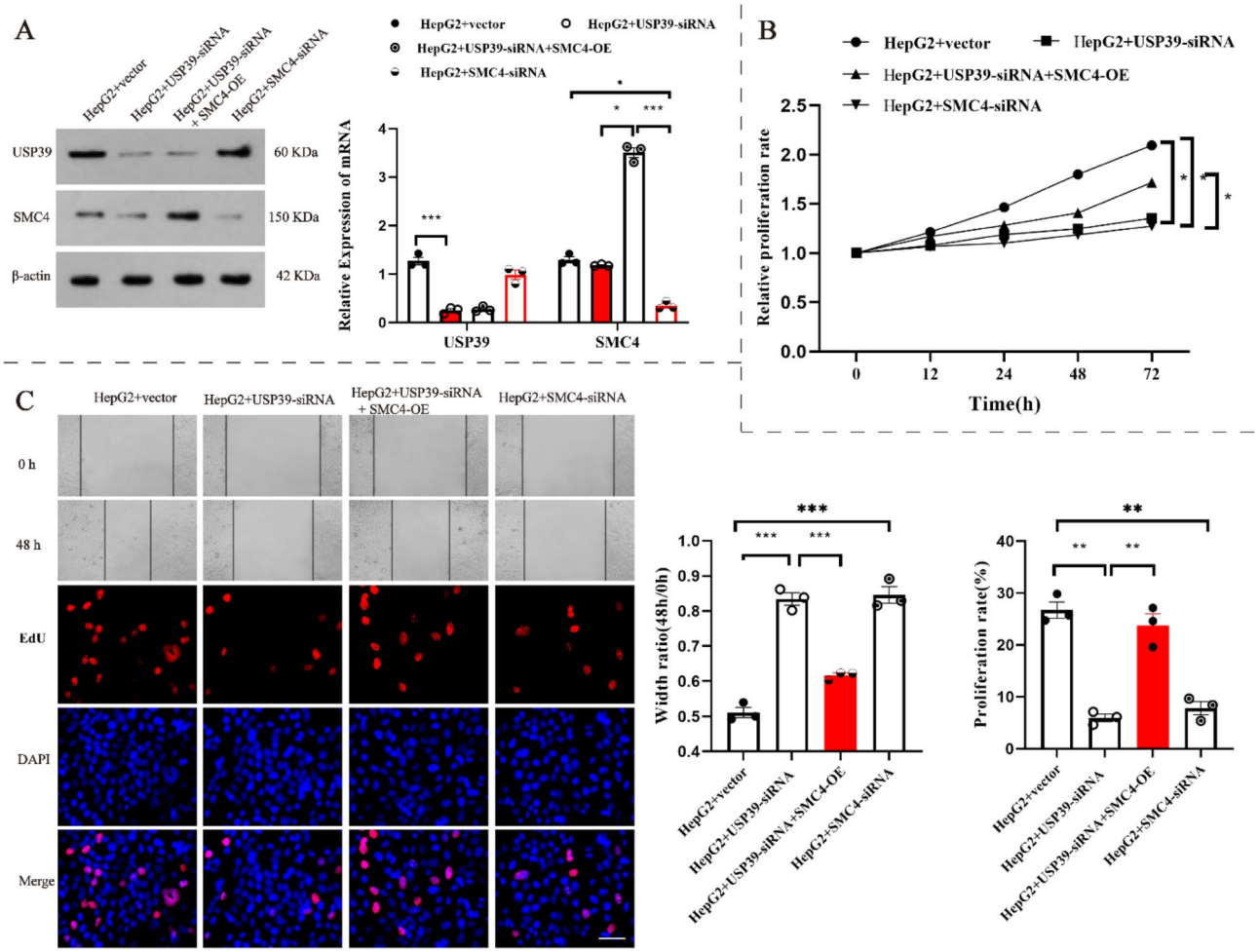

Fig. 4. USP39/SMC4 could promote the viability and proliferation of the HepG2 cells. Co-transfection experiments were conducted in HepG2 cells using USP39- siRNA and either SMC4-overexpression (OE) or SMC4-siRNA to investigate changes in cell phenotype. (**A**) qPCR and western blotting were performed to analyze the expression of USP39 and SMC4 after interfering, respectively. MTT(**B**), Scratch assay, and EdU (**C**) were used to detect the proliferation and viability of the HepG2 after USP39 and SMC4 interfering, respectively. (Data shown as mean ± SD; * $P < 0.05$, ** $P < 0.01$, *** $P < 0.001$; scale bar: 50 μm).

analysis was then performed on the 181 genes, identifying 24 genes (λ = 24) (Fig. S3A). Additionally, multivariate Cox regression analysis was conducted to construct risk models using the R (survival) package (Fig. S3A). Seven optimal genes (TIAL1, XPO1, ZNF207, STAT1, TBCCD1, LIMS1, and ATAD2) were selected for the model. Further, Risk scores were calculated, ranging from − 2.49 to 2.25, with an AIC of 0.73 and a p-value of 1.23×10^{-13} (Fig. S3B). The low-risk and high-risk groups were classified based on the median cutoff. Kaplan-Meier analysis was performed on the GSE14520 and TCGA-LIHC datasets, illustrating that the high-risk group exhibited shorter OS and RFS compared to the low-risk group (Fig. S3C). The risk score analysis revealed a higher death rate and shorter survival for the high-risk group compared to the low-risk group (Fig. S3D). From the LASSO regression and multivariate Cox analysis results using the GSE14520 dataset, TIAL1, ZNF207, LIMS1, and ATAD2 were identified as risk genes, whereas XPO1, STAT1, and TBCCD1 exhibited protective effects.

Kaplan-Meier analysis further revealed that high expression of ZNF207, TIAL1, and LIMS1, ATAD2(data not shown) was associated with poor prognosis of HCC (Fig. S4A). Furthermore, CHCC-HBV cohort validation confirmed that ZNF207 and TIAL1 were highly expressed in HCC (Fig. S4B), whereas LIMS1 exhibited showed low expression. No differential expression of ATAD2 was observed between the HCC and normal groups. Pearson correlation analysis also demonstrated a positive correlation between SMC4 and ZNF207, TIAL1, suggesting that SMC4 might regulate HCC progression through ZNF207 and TIAL1 (Fig. S4C).

To investigate the relationship between SMC4 and ZNF207, TIAL1, qPCR and western blotting assays were performed (Fig. 5A). The findings demonstrated a positive correlation expression between SMC4 and TIAL1, with TIAL1 expression increasing as SMC4 levels rose and decreasing as SMC4 expression decreased. In contrast, ZNF207 expression was unaffected by changes in SMC4 expression. These findings suggest that SMC4 could regulate the expression of TIAL1 but not ZNF207 at the gene and protein levels. To further explore functional alterations, HepG2 cells were subjected to upregulation of SMC4, combined with knockdown of TIAL1 or

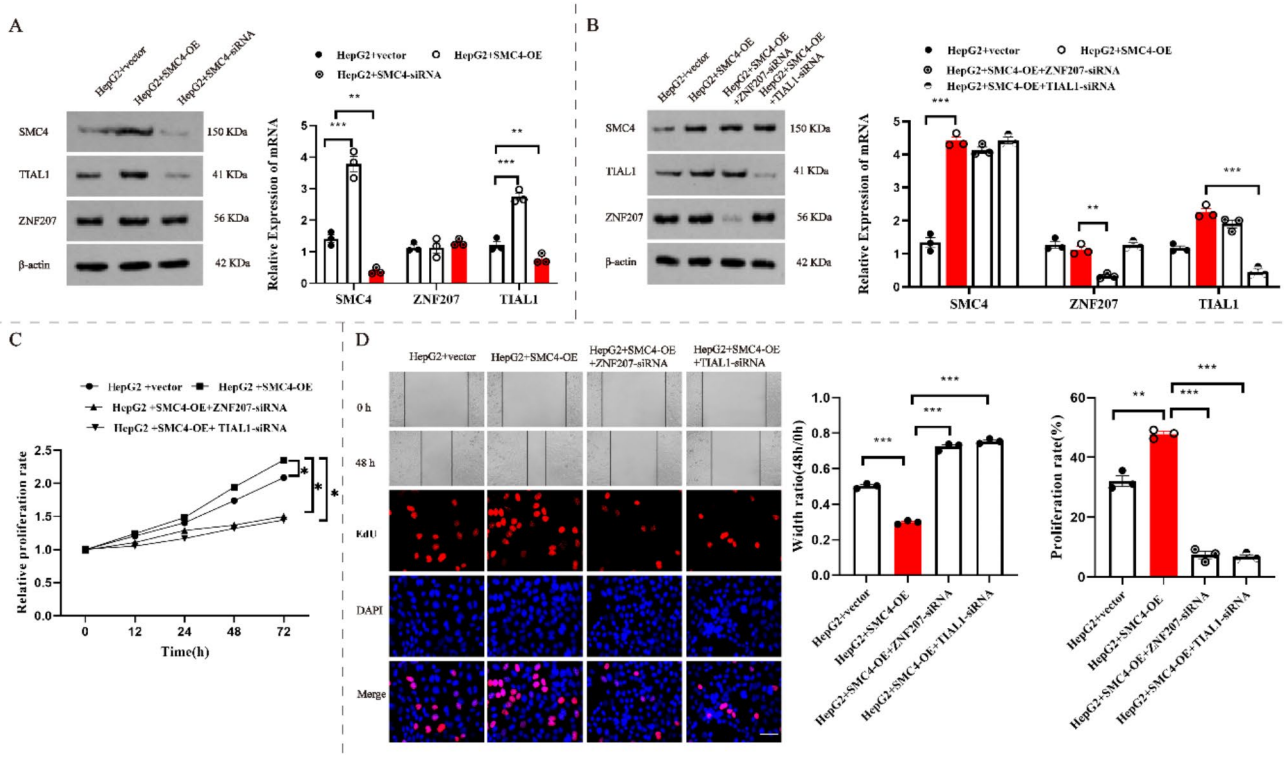

Fig. 5. SMC4 regulates the expression of TIAL1 and impacts the cell phenotype. (**A**) The relationship between SMC4 and ZNF207, TIAL1 was observed by qPCR and western blotting assays. (**B**)Western blotting and qPCR assays were applied to detect the changes in expression level after overexpression of SMC4 combined with ZNF207orTIAL1 knocking down, respectively. MTT (**C**), EdU, and Scratch assay (**D**) were used to detect the proliferation and viability of the HepG2 after overexpression of SMC4 combined with ZNF207 or TIAL1 knocking down, respectively. (Data shown as mean ± SD; * $P < 0.05$, ** $P < 0.01$, *** $P < 0.001$; scale bar: 50 μm).

ZNF207. qPCR and western blotting assays were applied to verify the effect of gene interference (Fig. 5B). MTT, EdU, and cell scratch assays were conducted to assess the proliferation and viability of HepG2 cells (Fig. 5C-D). The results demonstrated that the overexpression of SMC4 significantly enhanced the viability and proliferation of HepG2 cells (HepG2 + SMC4-OE). Conversely, when combined with TIAL1 or ZNF207 knockdown, the viability and proliferation of HepG2 cells were significantly reduced. These results suggest that SMC4, along with TIAL1 and ZNF207, collectively promotes the proliferation and viability of HepG2 cells.

SMC4 might regulate the drug resistance of hepatoma cell lines through TIAL1 and ZNF207

The R package(oncoPredict) was performed to predict IC50 based on both the GSE14520 and TCGA-LIHC datasets. The models were stratified into low-risk and high-risk groups based on the median risk score. The results suggested that higher expression of SMC4 was associated with elevated IC50 values in both the GSE14520 and TCGA-LIHC datasets, indicating that hepatoma cells in this group exhibited greater resistance to 5-FU (Fig. S5A-D).

We chose HepG2 cells, which showed the highest expression of SMC4, to generate drug-resistant cells. The MTT assay was used to assess the survival rate of HepG2 cells, and the IC50 value (723.083nM) was calculated at which cell proliferation inhibition reached 50% (Fig. 6A). Subsequently, these HepG2 cells were exposed to the determined concentration to develop drug-resistant cells, referred to as HepG2/ 5-FU. MTT and EdU assays were conducted to evaluate the viability and proliferation of HepG2 cells after overexpression of SMC4 and exposure to 5-FU (IC50, 723.083nM) for 24 h (Fig. 6B and C). The group (HepG2 + vector) served as the control group. In group (HepG2 + SMC4-OE), characterized by SMC4 overexpression, HepG2 cells exhibited decreased drug sensitivity and increased cell viability and proliferation compared to the (HepG2 + vector) group. In the (HepG2 + SMC4-OE + ZNF207- siRNA) and (HepG2 + SMC4-OE + TIAL1-siRNA) groups, SMC4 overexpression was combined with TIAL1 or ZNF207 knockdown. These interventions partially restored drug sensitivity and inhibited the viability and proliferation of HepG2 cells.

Additionally, MTT and EdU assays were also performed to assess the viability and proliferation of HepG2/5-FU cells following the knockdown of SMC4, TIAL1, and ZNF207, respectively (Fig. 6D and E). The (HepG2) and (HepG2/5-FU) group served as control groups. The results demonstrated that the HepG2/5-FU cells regained sensitivity to 5-FU after SMC4 knockdown in the (HepG2/5-FU + SMC4- siRNA) group. Similarly, in the (HepG2/5-FU + ZNF207-siRNA) and (HepG2/5- FU + TIAL1-siRNA) group, knockdown of TIAL1 or ZNF207 restored 5-FU sensitivity in HepG2/5-FU cells, inhibiting cell viability and proliferation. These findings

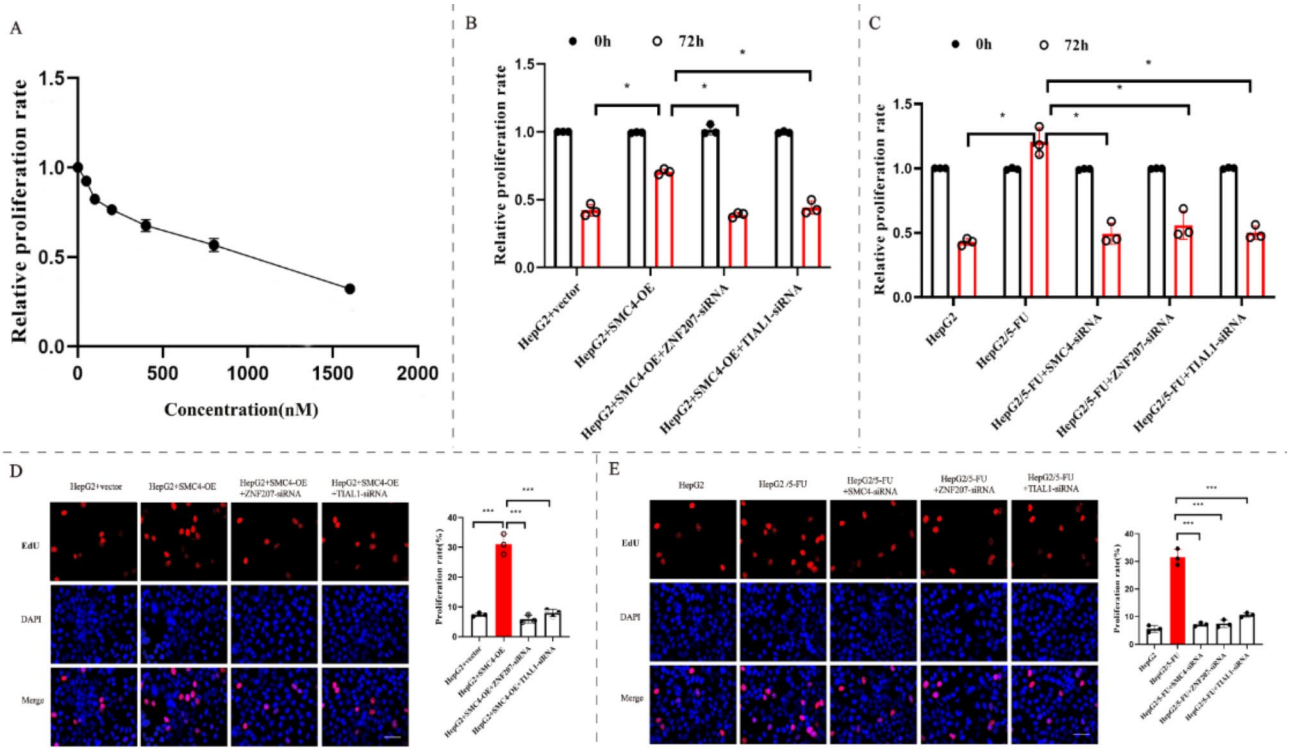

Fig. 6. SMC4 may regulate the drug resistance of hepatoma cell lines through TIAL1 and ZNF207. (**A**) The IC50 values of HepG2 were calculated using MTT assays. (**B**)MTT was applied to detect the proliferation of HepG2 after overexpression of SMC4 combined with ZNF207 or TIAL1 knocking down. (**C**) EdU was applied to detect the proliferation of HepG2 after overexpression of SMC4 combined with ZNF207 or TIAL1 knocking down. (**D**) MTT was applied to detect the proliferation of HepG2/5-FU after SMC4, ZNF207 and TIAL1 knocking down respectively. (**E**) EdU was applied to detect the proliferation of HepG2/5-FU after SMC4, ZNF207 and TIAL1 knocking down respectively. (Data shown as mean ± SD; * $P < 0.05$, ** $P < 0.01$, *** $P < 0.001$; scale bar: 50 μm).

suggest that SMC4 plays a key role in regulating drug resistance in hepatoma cell lines through its interaction with TIAL1 and ZNF207.

Discussion

With the deepening of our understanding of the molecular biology of HCC, numerous molecular targets associated with its occurrence and progression have been identified[30,31]. In addition to regulatory pathways, abnormal post-translational modification of many proteins, such as ubiquitin, SUMO, Neddylation, or cell dysfunction, all of which are linked to the onset and development of cancer[32,33]. Ubiquitination, in particular, is a crucial regulator of most signaling pathways, and disruptions in cell signaling are key drivers of cancer initiation, progression, and metastasis[34–36]. Deubiquitinating enzymes (DUBs) play essential roles in tumor regulation, acting as either tumor suppressors or oncogenes, and have emerged as promising therapeutic targets in cancer treatment[37–39].

In this study, we utilized bioinformatics to explore the role of SMC4 in HCC. We discovered that SMC4 undergoes significant amino acid modification, primarily through ubiquitination. Meanwhile, we observed a strong association between SMC4 ubiquitination and USP39. USP39, a member of the deubiquitinating enzyme family, features a central zinc-finger ubiquitin-binding domain and a ubiquitin c-terminal hydrolase domain[40]. Growing evidence indicates that abnormal expression of USP39 contributes to tumorigenesis and is linked to HCC progression[41–43]. Further, experimental validation confirmed that USP39-siRNA promotes SMC4 ubiquitination, leading to a decrease in SMC4 protein levels. Subsequent investigations revealed that USP39 hinders the ubiquitination process, thereby preserving the stability of SMC4 and inhibiting its protein degradation.

Next, we used bioinformatics to develop a seven-gene prognostic model related to the SMC4, ZNF207, and TIAL1, all of which were ultimately selected for further study. T-cell intracellular antigen 1-related/like (TIAR/TIAL1) protein, a well-known member of the RNA-binding protein (RBP) family, is considered an unfavorable prognostic marker in HCC[44,45]. Zinc finger protein 207 (ZNF207), a member of the ZNF protein family, is upregulated in hepatoma cells and associated with poor prognosis[46–48].Experimental results showed that ZNF207-siRNA could reduce cell proliferation and scratch repair ability due to the SMC4-OE. And the SMC4-OE had no effect on the expression of ZNF207. This suggests that SMC4 does not affect ZNF207 at the gene and protein expression levels, implying potential protein-protein interactions or other intracellular interactions.

We also found that TIAL1 expression could be influenced by the level of SMC4 expression. Meanwhile, TIAL1-siRNA can reduce the cell proliferation and scratch repair ability induced by SMC4-OE, indicating that SMC4 may regulate the expression of TIAL1 and that the function of SMC4 is partially achieved through the mediation of ZNF207. Our findings collectively demonstrate that SMC4 promotes the growth and survival of hepatoma cells, likely through activation of the ZNF207 and TIAL1 pathways.

Additionally, we investigated the effect of SMC4 on the resistance of hepatoma cells to 5-FU by establishing drug-resistant HepG2/5-FU cell lines. Our results showed that overexpression of SMC4 reduced the sensitivity of HepG2/5-FU cells to 5-FU, thereby enhancing cell proliferation. Interfering with the expression of SMC4, TIAL1, and ZNF207 restored the sensitivity of HepG2/5-FU cells to 5-FU and inhibited cell growth. Taken together with previous findings, we conclude that SMC4 plays a role in regulating drug resistance in HCC cells, likely through the TIAL1 and ZNF207 pathways.

Conclusions

Our study provides valuable insights into the important role of USP39 in SMC4 deubiquitination modification, which contributes to maintaining the protein's level. Furthermore, we provide evidence that SMC4 might promote hepatoma cells' proliferation and drug resistance through the TIAL1 and ZNF207 pathways. These findings offer potential therapeutic targets for HCC patients, particularly those with elevated SMC4 expression levels.

Data availability

The datasets generated and/or analyzed during the current study are available from the corresponding author upon reasonable request.

Received: 31 July 2024; Accepted: 4 March 2025
Published online: 14 March 2025

References

1. Chidambaranathan-Reghupaty, S., Fisher, P. B. & Sarkar, D. Hepatocellular carcinoma (HCC): epidemiology, etiology and molecular classification. *Adv. Cancer Res.***149**, 1–61 (2021).
2. Piñero, F., Dirchwolf, M. & Pessôa, M. G. Biomarkers in hepatocellular carcinoma: diagnosis, prognosis and treatment response assessment. *Cells***9** (6), 1370 (2020).
3. Kim, E. & Viatour, P. Hepatocellular carcinoma: old friends and new tricks. *Exp. Mol. Med.***52** (12), 1898–1907 (2020 Dec).
4. Sung, H. et al. Global Cancer statistics 2020: GLOBOCAN estimates of incidence and mortality worldwide for 36 cancers in 185 countries. *CA Cancer J. Clin.***71** (3), 209–249 (2021).
5. Brown, Z. J. et al. Management of hepatocellular carcinoma: A review. *JAMA Surg.***158** (4), 410–420 (2023).
6. Gilles, H., Garbutt, T. & Landrum, J. Hepatocellular carcinoma. *Crit. Care Nurs. Clin. North. Am.***34** (3), 289–301 (2022).
7. Calderaro, J., Seraphin, T. P., Luedde, T. & Simon, T. G. Artificial intelligence for the prevention and clinical management of hepatocellular carcinoma. *J. Hepatol.***76** (6), 1348–1361 (2022).
8. Villanueva, A. & Hepatocellular Carcinoma *N Engl. J. Med.***380**(15):1450–1462 (2019).
9. Yang, J. D. et al. A global view of hepatocellular carcinoma: trends, risk, prevention and management. *Nat. Rev. Gastroenterol. Hepatol.***16** (10), 589–604 (2019).
10. Sidali, S., Trépo, E., Sutter, O. & Nault, J. C. New concepts in the treatment of hepatocellular carcinoma. *United Eur. Gastroenterol. J.***10** (7), 765–774 (2022).
11. Zhou, H. & Song, T. Conversion therapy and maintenance therapy for primary hepatocellular carcinoma. *Biosci. Trends*. **15** (3), 155–160 (2021).
12. Zhu, K. et al. Medium or large hepatocellular carcinoma: Sorafenib combined with transarterial chemoembolization and radiofrequency ablation. *Radiology***288** (1), 300–307 (2018).
13. Vogel, A., Meyer, T., Sapisochin, G., Salem, R. & Saborowski, A. *Hepatocellular Carcinoma Lancet***400**(10360):1345–1362 (2022).
14. Xie, D. Y. et al. A review of 2022 Chinese clinical guidelines on the management of hepatocellular carcinoma: updates and insights. *Hepatobiliary Surg. Nutr.***12** (2), 216–228 (2023).
15. Koide, H., Kodera, N., Bisht, S., Takada, S. & Terakawa, T. Modeling of DNA binding to the condensin hinge domain using molecular dynamics simulations guided by atomic force microscopy. *PloS Comput. Biol.***17** (7), e1009265 (2021).
16. Ryu, J. K. et al. The condensin holocomplex cycles dynamically between open and collapsed States. *Nat. Struct. Mol. Biol.***27** (12), 1134–1141 (2020).
17. Cobbe, N. & Heck, M. M. SMCs in the world of chromosome biology: from prokaryotes to eukaryotes. *J. Struct. Biol.***129**, 123–143 (2000).
18. Wang, H., Liu, Y., Yuan, J., Zhang, J. & Han, F. The condensin subunits SMC2 and SMC4 interact for correct condensation and segregation of mitotic maize chromosomes. *Plant. J.***102** (3), 467–479 (2020).
19. Thadani, R., Uhlmann, F. & Heeger, S. Condensin, chromatin crossbarring and chromosome condensation. *Curr. Biol.***22** (23), R1012–R1021 (2012).
20. Zhou, B. et al. A novel miR-219-SMC4- JAK2/Stat3 regulatory pathway in human hepatocellular carcinoma. *J. Exp. Clin. Cancer Res.***33**, 55 (2014).
21. Zhang, S. R. et al. SMC4 enhances the chemoresistance of hepatoma cells by promoting autophagy. *Ann. Transl Med.***10** (24), 1308 (2022).
22. Sun, X. et al. The diapause-like colorectal cancer cells induced by SMC4 Attenuation are characterized by low proliferation and chemotherapy insensitivity. *Cell. Metab.***35** (9), 1563–1579e8 (2023).
23. Yan, Y. et al. SMC4 knockdown inhibits malignant biological behaviors of endometrial cancer cells by regulation of FoxO1 activity. *Arch. Biochem. Biophys.***712**, 109026 (2021).
24. Huang, M. L., Shen, G. T. & Li, N. L. Emerging potential of ubiquitin-specific proteases and ubiquitin -specific proteases inhibitors in breast cancer treatment. *World J. Clin. Cases*. **10** (32), 11690–11701 (2022).
25. Bidkhori, G. et al. Reconstruction of an integrated genome-scale co-expression network reveals key modules involved in lung adenocarcinoma. *PloS One*. **8** (7), e67552 (2013).
26. Zhao, Z., Wang, X., Ding, Y., Cao, X. & Zhang, X. SMC4, a novel tumor prognostic marker and potential tumor therapeutic target. *Front. Oncol.***13**, 1117642 (2023).
27. Cheng, Z. et al. HBV-infected hepatocellular carcinoma can be robustly classified into three clinically relevant subgroups by a novel analytical protocol. *Brief. Bioinform*. **24** (2), bbac601 (2023).

28. Nie, H. et al. Clinical significance and integrative analysis of the SMC family in hepatocellular carcinoma. *Front. Med. (Lausanne).* **8**, 727965 (2021).
29. Jin, M. et al. ZNF131 facilitates the growth of hepatocellular carcinoma by acting as a transcriptional activator of SMC4 expression. *Biochem. Biophys. Res. Commun.***696**, 149515 (2024).
30. Juaid, N. et al. Anti-Hepatocellular carcinoma biomolecules: molecular targets insights. *Int. J. Mol. Sci.***22** (19), 10774 (2021).
31. Wang, Y. & Deng, B. Hepatocellular carcinoma: molecular mechanism, targeted therapy, and biomarkers. *Cancer Metastasis Rev.***42** (3), 629–652 (2023).
32. Wang, Y. & Chen, H. Protein glycosylation alterations in hepatocellular carcinoma: function and clinical implications. *Oncogene***42**, 1970–1979 (2023).
33. Pellegrino, N. E. et al. The next frontier: translational development of ubiquitination, sumoylation, and neddylation in Cancer. *Int. J. Mol. Sci.***23** (7), 3480 (2022).
34. Hershko, A. & Ciechanover, A. The ubiquitin system. *Annu. Rev. Biochem.***67**, 425–479 (1998).
35. Cockram, P. E. et al. Ubiquitination in the regulation of inflammatory cell death and cancer. *Cell. Death Differ.***28**, 591–605 (2021).
36. Liu, F. et al. Ubiquitination and deubiquitination in cancer: from mechanisms to novel therapeutic approaches. *Mol. Cancer*. **23** (1), 148 (2024).
37. Dewson, G., Eichhorn, P. J. A. & Komander, D. Deubiquitinases in cancer. *Nat. Rev. Cancer*. **23** (12), 842–862 (2023).
38. Sun, T., Liu, Z. & Yang, Q. The role of ubiquitination and deubiquitination in cancer metabolism. *Mol. Cancer*. **19** (1), 146 (2020).
39. Han, S. et al. The role of ubiquitination and deubiquitination in tumor invasion and metastasis. *Int. J. Biol. Sci.***18** (6), 2292–2303 (2022).
40. Zhao, Y. et al. Knockdown of USP39 induces cell cycle arrest and apoptosis in melanoma. *Tumour Biol.***37**, 13167–13176 (2016).
41. Wang, L. et al. USP39 promotes ovarian cancer malignant phenotypes and carboplatin chemoresistance. *Int. J. Oncol.***55**, 277–288 (2019).
42. Yuan, X. et al. USP39 promotes the growth of human hepatocellular carcinoma in vitro and in vivo. *Oncol. Rep.***34**, 823–832 (2015).
43. Wang, W. et al. USP39 stabilizes β-catenin by deubiquitination and suppressing E3 ligase TRIM26 pre-mRNA maturation to promote HCC progression. *Cell. Death Dis.***14** (1), 63 (2023).
44. Izquierdo, J. M. et al. Knockdown of T-cell intracellular antigens triggers cell proliferation, invasion and tumour growth. *Biochem. J.***435**, 337–344 (2011).
45. Chen, J. et al. MBNL1 suppressed cancer metastatic of skin squamous cell carcinoma via by TIAL1/MYOD1/caspase-9/3 signaling pathways. *Technol. Cancer Res. Treat.***20**, 1533033820960755 (2021).
46. Pahl, P. M. et al. ZNF207, a ubiquitously expressed zinc finger gene on chromosome 6p21.3. *Genomics***53** (3), 410–412 (1998).
47. Fang, F. et al. A distinct isoform of ZNF207 controls self-renewal and pluripotency of human embryonic stem cells. *Nat. Commun.***9** (1), 4384 (2018).
48. Wang, X. et al. System analysis based on the cancer-immunity cycle identifies ZNF207 as a novel immunotherapy target for hepatocellular carcinoma. *J. Immunother Cancer*. **10** (3), e004414 (2022).

Acknowledgements

The study was conducted according to the guidelines of the Declaration of Helsinki, and approved by the Ethics Committee of Daping Hospital, Army Medical University ((2022) No.229). Written informed consent was obtained from all patients.

Author contributions

G. C. and J. C. is responsible for designing the research project; B.Z. is responsible for writing the manuscript and data analysis; J. L.and S. W. is responsible for collecting patient samples; H. Z. and Y. L. is responsible for conducting experiments.All authors reviewed the manuscript.

Funding

This study was supported by the Science and Technology Research Program of Chongqing Municipal education Commission (KJZD-K202412801).

Declarations

Competing interests

The authors declare no competing interests.

Additional information

Supplementary Information The online version contains supplementary material available at https://doi.org/10.1038/s41598-025-93029-x.

Correspondence and requests for materials should be addressed to J.C. or G.C.

Reprints and permissions information is available at www.nature.com/reprints.

Publisher's note Springer Nature remains neutral with regard to jurisdictional claims in published maps and institutional affiliations.

Open Access This article is licensed under a Creative Commons Attribution-NonCommercial-NoDerivatives 4.0 International License, which permits any non-commercial use, sharing, distribution and reproduction in any medium or format, as long as you give appropriate credit to the original author(s) and the source, provide a link to the Creative Commons licence, and indicate if you modified the licensed material. You do not have permission under this licence to share adapted material derived from this article or parts of it. The images or other third party material in this article are included in the article's Creative Commons licence, unless indicated otherwise in a credit line to the material. If material is not included in the article's Creative Commons licence and your intended use is not permitted by statutory regulation or exceeds the permitted use, you will need to obtain permission directly from the copyright holder. To view a copy of this licence, visit http://creativecommons.org/licenses/by-nc-nd/4.0/.

© The Author(s) 2025